2 Chemical shifts

2.1 Introduction

The NMR frequency of a nucleus in a molecule is determined principally by its magnetogyric ratio, γ, and the strength, B, of the magnetic field it experiences (eqn 1.10):

$$\nu_{\mathrm{NMR}} = \frac{|\gamma| B}{2\pi}. \tag{2.1}$$

Thus, ^{1}H and ^{13}C nuclei resonate respectively at 400 and 100.6 MHz in a 9.4 T field. But not all protons, nor all carbons, have identical resonance frequencies: ν_{NMR} depends (slightly) on the position of the nucleus in the molecule, or to be more precise, on the local electron distribution. This effect, the *chemical shift*, is one of the things that makes NMR so attractive to chemists. It makes it possible to distinguish, for example, the three kinds of hydrogen atoms in ethanol (Fig. 1.1) and gives separately detectable signals for the hundreds of hydrogen atoms in a protein (Fig. 2.1).

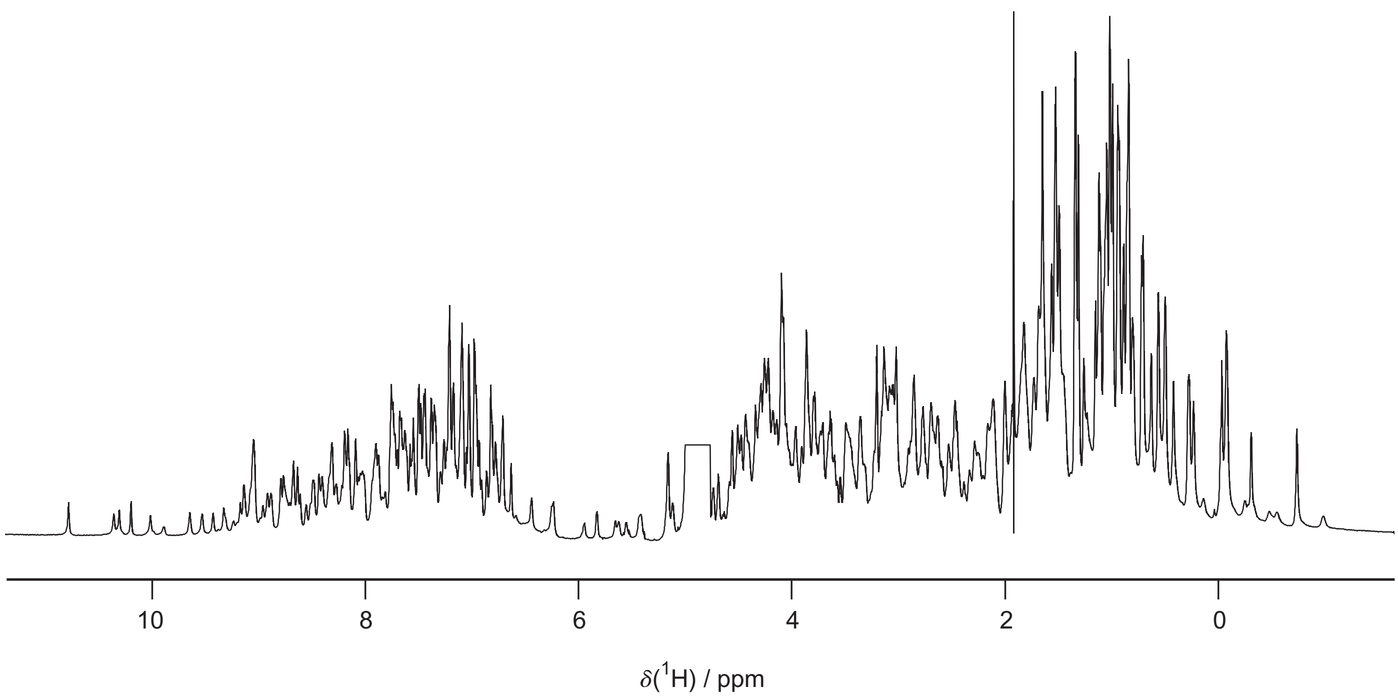

Fig. 2.1 950 MHz ^{1}H spectrum of hen egg-white lysozyme in H_2O. This protein has 129 amino acid residues and a relative molecular mass of ~14,500. The resonance of the solvent protons at ~4.7 ppm has been truncated. This spectrum was kindly provided by C. Redfield.

2.2 Nuclear shielding

Chemical shifts arise because the field, B, actually experienced by a nucleus in an atom or molecule differs slightly from the external field, B_0, produced by the magnet. B_0 is the field that would be felt by a bare nucleus, stripped of its electrons. In an atom, B is slightly smaller than B_0 because the external field causes the electrons to circulate within their atomic orbitals; this induced motion, much like an electric current passing through a coil of wire, generates a small magnetic field B' in the *opposite* direction to B_0 (Fig. 2.2). The nucleus is thus said to be *shielded* from the external field by its surrounding electrons ($B = B_0 - B'$).

B' is proportional to B_0 (the stronger the external field, the more it 'stirs up' the electrons) and typically 10^4–10^5 times smaller. Thus, the field at the nucleus may be written

$$B = B_0(1-\sigma) \tag{2.2}$$

where σ, the constant of proportionality between B' and B_0, is called the *shielding constant* or *screening constant*. As a result of nuclear shielding, the resonance condition (eqn 2.1) becomes

$$\nu_{\mathrm{NMR}} = \frac{|\gamma| B_0}{2\pi}(1-\sigma), \tag{2.3}$$

i.e. the resonance frequency of a nucleus in an atom is slightly lower than that of a bare nucleus, stripped of all its electrons (Fig. 2.3).

Similar effects occur for nuclei in molecules, except that the motion of the electrons is rather more complicated than in atoms with the result that the induced fields may *augment* or *oppose* the external field. Nevertheless, the effect is still referred to as nuclear shielding. Both the size and sign of the shielding constant in eqn 2.3 are determined by the electronic structure of the molecule in the vicinity of the nucleus. The resonance frequency of a nucleus is therefore characteristic of its environment.

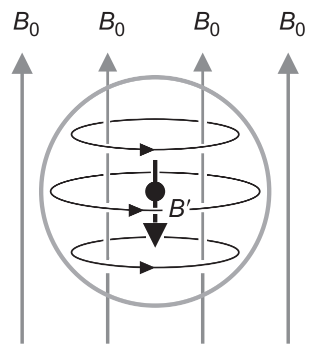

Fig. 2.2 An applied magnetic field B_0 causes the electrons in an atom to circulate within their orbitals. This motion generates an extra field B' which opposes B_0 and results in a net field $B = B_0 - B'$ at the site of the nucleus.

Larmor frequency

As mentioned briefly at the end of Chapter 1, the signal in an NMR experiment arises from the motion of the magnetization of the sample in the strong magnetic field of the spectrometer. Consider a collection of identical, non-interacting nuclear spins experiencing a magnetic field $\boldsymbol{B}$. The *magnetization vector* $\boldsymbol{M}$ (the sum of the magnetic moment vectors of the individual spins) moves as shown in Fig. 2.4. It *precesses* around $\boldsymbol{B}$, maintaining a constant angle with respect to $\boldsymbol{B}$ and therefore a constant projection onto $\boldsymbol{B}$. This motion, akin to that of the axis of a spinning top or gyroscope, is known as *Larmor precession*. The frequency of this motion, known as the *Larmor frequency*, is given by

$$\nu_0 = -\frac{\gamma B_0}{2\pi}(1-\sigma) \tag{2.4}$$

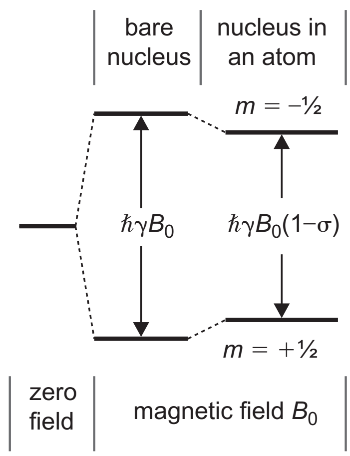

Fig. 2.3 Energy levels of a spin-$\frac{1}{2}$ nucleus with $\gamma > 0$. The energy-level splitting for a nucleus in an atom equals $h\nu_{\mathrm{NMR}}$ where ν_{NMR} is given by eqn 2.3.

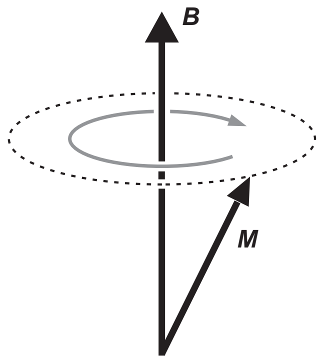

Fig. 2.4 Larmor precession of the magnetization vector ***M*** of nuclear spins with a positive magnetogyric ratio ($\gamma > 0$) and hence negative Larmor frequency ($\nu_0 < 0$) in a magnetic field ***B***. When $\gamma < 0$, ***M*** precesses in the opposite sense.

ν_0 is negative for nuclei with $\gamma > 0$, e.g. ^{1}H and ^{13}C, and positive for those with $\gamma < 0$, e.g. ^{15}N and ^{29}Si (Table 1.3). The sign of ν_0 determines the sense of the Larmor precession (clockwise or anticlockwise), as indicated in Fig. 2.4. From eqns 2.3 and 2.4, $\nu_0 = -\nu_{NMR}$ for spins with positive γ and $\nu_0 = \nu_{NMR}$ for those with negative γ. Remember that ν_{NMR} was defined (eqn 1.10) as the energy-level spacing ΔE divided by Planck's constant and is always positive. Larmor precession is discussed in more detail in Chapter 6.

Throughout this book, the Greek letter *nu* (e.g. in ν_0 and ν_{NMR}) is used as the symbol for frequencies expressed in hertz (Hz) or equivalently cycles per second or simply s^{-1}. From time to time we will also use the Greek letter *omega* (ω) for *angular* frequencies which have dimensions of radians per second (rad s^{-1}). The two types of frequency differ by a factor of 2π. So, for example, the Larmor angular frequency is given by

$$\omega_0 = 2\pi\nu_0 = -\gamma B_0(1-\sigma) \tag{2.5}$$

Defining chemical shifts

The shielding constant σ is an inconvenient measure of the chemical shift. Since absolute shifts are rarely needed and difficult to determine, it is common practice to define the chemical shift in terms of the *difference* between the Larmor frequency of the nucleus of interest (ν_0) and that of a reference nucleus ($\nu_{0,ref}$) using the dimensionless parameter δ:

$$\delta = 10^6\left(\frac{\nu_0 - \nu_{0,\mathrm{ref}}}{\nu_{0,\mathrm{ref}}}\right). \tag{2.6}$$

The frequency difference $\nu_0 - \nu_{0,ref}$ is divided by $\nu_{0,ref}$ so that δ is independent of the strength of the magnetic field used to measure it. The factor of 10^6 simply scales the numerical value of δ to a more convenient size: δ values are quoted in *parts per million*, or ppm.

To see how δ is related to the shielding constants, eqns 2.4 and 2.6 can be combined to give

$$\delta = 10^6\left(\frac{\sigma_{\mathrm{ref}} - \sigma}{1-\sigma_{\mathrm{ref}}}\right) \approx 10^6(\sigma_{\mathrm{ref}} - \sigma) \tag{2.7}$$

where $\sigma_{ref} \ll 1$ has been used. The larger the value of σ (greater shielding) the smaller the chemical shift. δ is therefore a *deshielding* parameter.

The reference signal is most conveniently obtained by adding a small amount of a suitable compound to the NMR sample. For ^{1}H and ^{13}C spectra this is usually tetramethylsilane $(CH_3)_4Si$, known as TMS. This molecule is inert, soluble in most organic solvents, and gives a single, strong ^{1}H resonance from its 12 identical protons. Moreover, both the ^{1}H and ^{13}C nuclei in TMS are quite strongly shielded (large shielding constant), with the result that most ^{1}H and ^{13}C chemical shifts are positive numbers ($\delta > 0$).

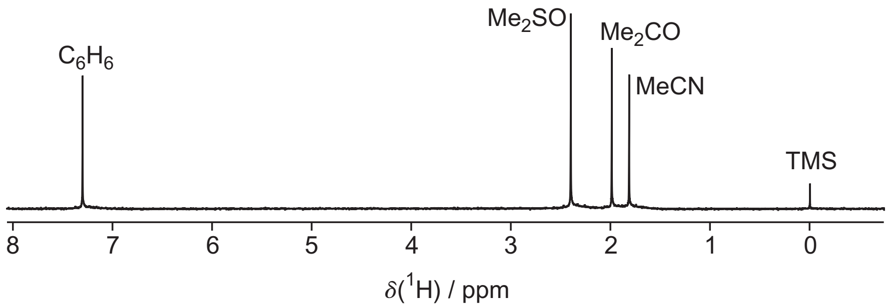

Fig. 2.6 400 MHz ^{1}H NMR spectrum of a mixture of benzene, dimethylsulphoxide, acetone, acetonitrile, and tetramethylsilane.

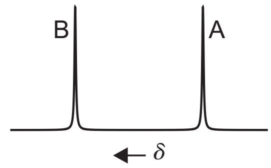

Fig. 2.5 NMR spectra are conventionally plotted with the chemical shift δ increasing from right to left. Spin A is more strongly shielded (larger σ) than spin B and so appears to the right of B in the spectrum. For spins with $\gamma > 0$, A has a less negative, i.e. larger, ν_0 than B.

Conventionally, NMR spectra are plotted with δ increasing from right to left. Thus, more heavily shielded nuclei (larger σ, smaller δ) appear towards the right-hand side of the spectrum (Fig. 2.5).

As a simple example, Fig. 2.6 shows the 400 MHz ^{1}H spectrum of a mixture of compounds with a small amount of TMS added. Each of the five molecules has a single group of identical protons, and hence a single chemical shift. Notice that the chemical shift scale covers about 10 ppm, a typical range for ^{1}H. Chemical shifts can easily be converted back into frequencies using eqn 2.6. For example, the acetone peak in Fig. 2.6 has $\delta = 2.0$ ppm, so that

$$\begin{aligned} \left|\nu_{0,\text{acetone}} - \nu_{0,\text{TMS}}\right| &= \left(\delta / 10^6\right)\left|\nu_{0,\text{TMS}}\right| \\ &= \left(2.0 \times 10^{-6}\right) \times \left(400\,\text{MHz}\right) = 800\,\text{Hz}. \end{aligned} \tag{2.8}$$

On a 100 MHz spectrometer, the chemical shift of acetone is still 2.0 ppm, but the Larmor frequency relative to TMS is reduced proportionately to 200 Hz.

Examples

As we shall see later, so many factors play a role in determining the size of chemical shifts that it is often difficult to relate experimental measurements *quantitatively* to molecular structure. However, valuable information can often be extracted from NMR spectra simply by noting the number of resonances and their relative intensities, as the examples in the following paragraphs illustrate.

In CS_2 solution, phosphorus pentachloride has a single ^{31}P resonance (Fig. 2.7), as might be expected from the trigonal bipyramidal structure found in the gas phase. Solid phosphorus pentachloride, however, has *two* equally intense ^{31}P peaks, revealing clearly that the change of phase is accompanied by a change in structure (actually the disproportionation reaction $2PCl_5 \rightarrow PCl_6^- + PCl_4^+$).

The ^{17}O NMR spectrum of $Co_4(CO)_{12}$ in chloroform at low temperature comprises four equally intense lines (Fig. 2.8), consistent with a bridged structure (C_{3v} symmetry) containing four distinct types of carbonyl. This spectrum clearly rules out a non-bridged $Ir_4(CO)_{12}$-type structure (T_d symmetry), in which all 12 carbonyls are in identical environments. It also provides strong evidence against the D_{2d} structure at one time proposed for $Co_4(CO)_{12}$ in which there are only *three* distinct carbonyl environments: one bridging and two terminal.

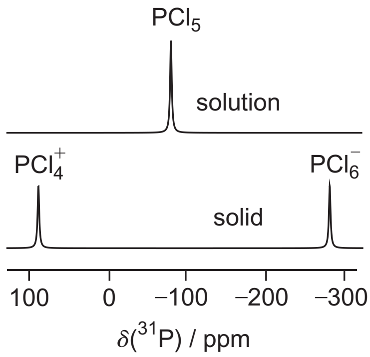

Fig. 2.7 ^{31}P NMR spectra of phosphorus pentachloride in the solid state and in solution in CS_2. The former was obtained using a technique known as *magic angle spinning* to remove the large linebroadening caused by, amongst other things, the dipolar interactions (Section 3.8 and Appendix A) between nuclei in the solid. The chemical shift reference is an 85% aqueous solution of orthophosphoric acid. (Adapted from E. R. Andrew, *Phil. Trans. R. Soc. A*, **299** (1981) 505.)

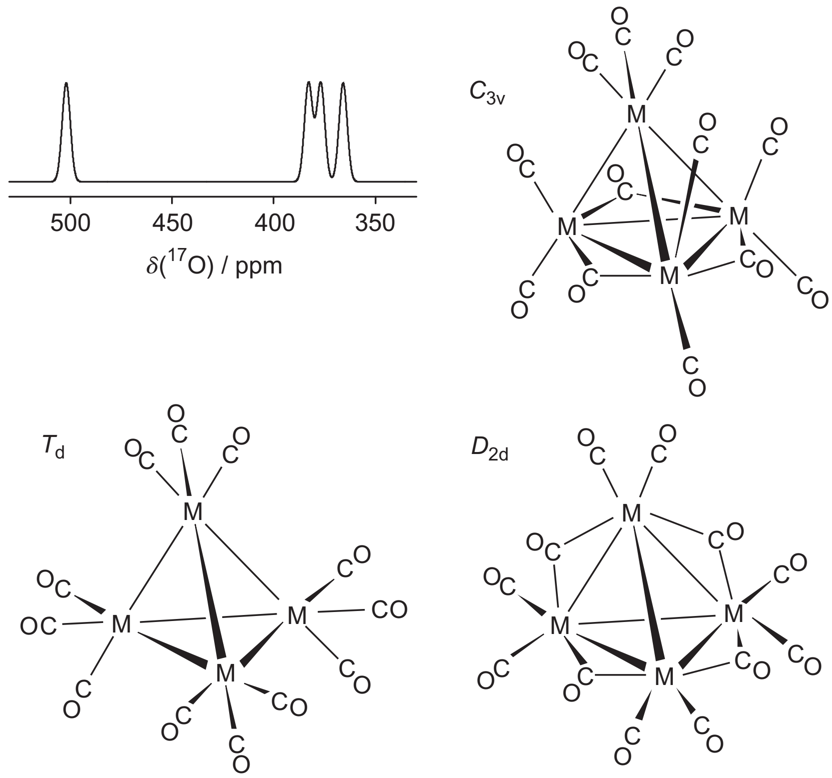

Fig. 2.8 The ^{17}O NMR spectrum of $Co_4(CO)_{12}$ in chloroform at −25 °C is consistent with the C_{3v} structure shown, but not the T_d or D_{2d} forms.

Occasionally, structural information can be deduced solely from the relative intensities of NMR lines. For example, the only possible structures for the compounds C_9H_{12} and $C_{10}H_{14}$ with the ^1H spectra shown in Fig. 2.9 are 1,3,5-trimethylbenzene and 1,2,4,5-tetramethylbenzene, respectively.

A dramatic illustration of the use of chemical shifts is provided by the ^{13}C NMR spectrum of the fullerene C_{60} (Fig. 2.10). The observation of a single NMR line for this remarkable molecule provides direct evidence for its highly symmetrical football-like structure in which all 60 carbon atoms are in identical environments.

Zeolites are aluminosilicates built from corner-sharing SiO_4 and AlO_4 tetrahedra. Each silicate and aluminate group is linked, via oxygen bridges, to four

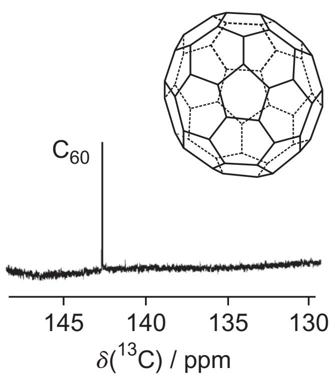

Fig. 2.10 ^{13}C NMR spectrum of C_{60}. (Adapted from R. Taylor, J. P. Hare, A. K. Abdul-Sada, and H. W. Kroto, *J. Chem. Soc. Chem. Commun.* (1990) 1423.)

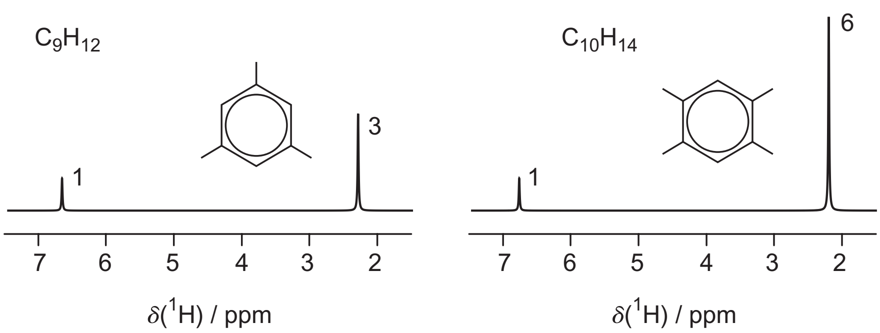

Fig. 2.9 ^1H spectra of compounds with molecular formulae C_9H_{12} and $C_{10}H_{14}$. The relative intensities of the peaks, obtained by integration, are as shown.

other tetrahedra to give framework structures containing cavities and channels, which confer useful catalytic properties. Up to five distinct chemical shifts can be observed in the ^{29}Si NMR spectra of powdered zeolites (Fig. 2.11), corresponding to Si atoms linked to n AlO_4 tetrahedra and $(4-n)$ SiO_4 tetrahedra, with $n = 0-4$. Each Al atom shifts the Si resonance by roughly +5 ppm. The relative intensities of the five peaks give the Si/Al ratio, and can be used to test model structures with different Si/Al ordering patterns.

Chemical shifts may be interpreted empirically using data derived from compounds of known structure. For example, Fig. 2.12 shows typical ^{1}H chemical shift ranges for assorted organic functional groups. When combined with empirical rules for predicting substituent effects (see e.g. Friebolin (2011), Günther (2013), and Williams and Fleming (2007)), such tables can be extremely useful in making connections between observed shifts and molecular structures. However, as NMR techniques become ever more sophisticated (Chapter 6), such methods generally become less important. More direct structural information is often provided by spin–spin couplings (Chapter 3) and nuclear Overhauser effects (Chapter 5).

Finally, a somewhat different use of chemical shifts is illustrated by the pH dependence of the ^{1}H spectrum of the amino acid histidine (Fig. 2.13). The resonance frequencies of the H2 and H4 protons in the imidazole group change smoothly with pH between the chemical shifts of the charged form $HisH^+$, stable in acidic solution, and those of the neutral, deprotonated form His, which is present at high pH. At any pH, the observed chemical shift is a weighted average of the two extreme values δ_{HisH^+} and δ_{His}:

$$\delta = \frac{\delta_{HisH^+}[HisH^+] + \delta_{His}[His]}{[HisH^+] + [His]}$$

where $[HisH^+]$ and [His] are the concentrations. The details of this averaging process are discussed in Chapter 4. The midpoint of the titration occurs when

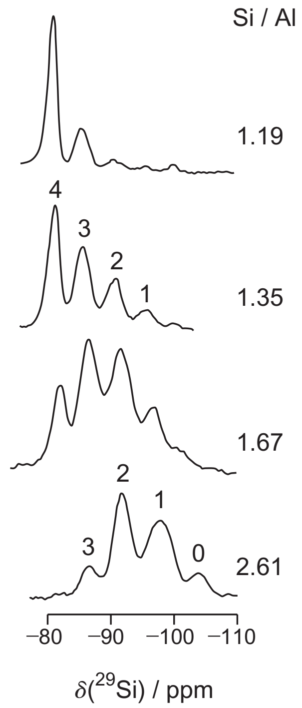

Fig. 2.11 ^{29}Si NMR spectra of synthetic zeolites recorded with magic angle spinning. The resonances of Si atoms linked to n AlO_4 tetrahedra and $(4-n)$ SiO_4 tetrahedra are labelled $n = 0-4$. The Si/Al ratios are as indicated. (Adapted from J. Klinowski, S. Ramdas, J. M. Thomas, C. A. Fyfe, and J. S. Hartman, *J. Chem. Soc. Faraday Trans. II*, **78** (1982) 1025.)

Figures 2.7–2.9 and several others in subsequent chapters show NMR spectra that have been drawn on a computer so as to resemble the original experimental spectra (references to which are normally given in the figure captions). Genuine spectra, e.g. Figs 2.6, 2.10, and 2.11, can be recognized as such by the presence of noise.

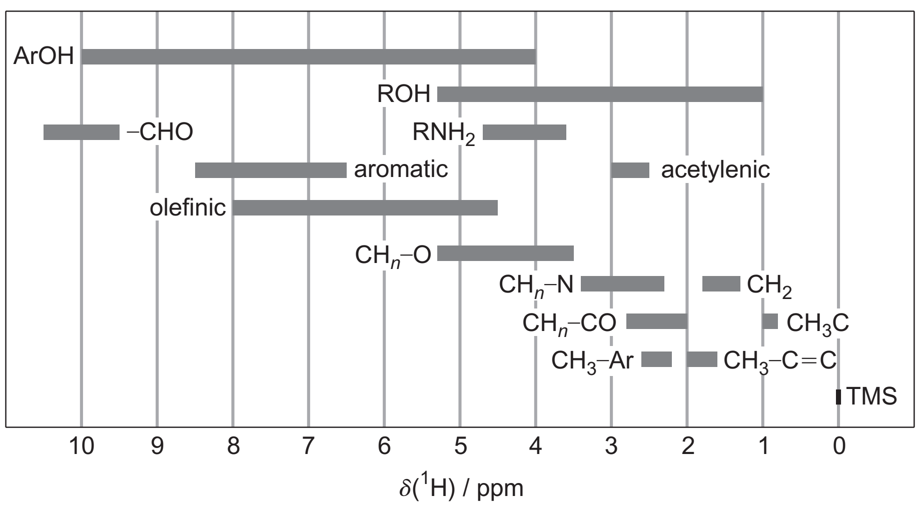

Fig. 2.12 Typical ^{1}H chemical shift ranges for some common organic functional groups relative to the reference compound tetramethylsilane ($\delta = 0$ ppm).

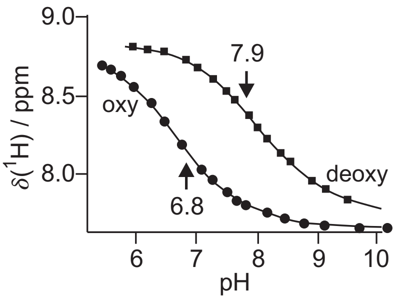

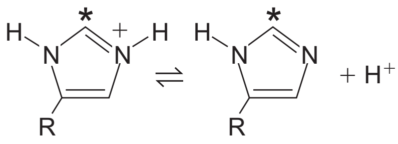

Fig. 2.13 The chemical shift of the H2 proton (asterisked) of histidine β146 in oxy- and deoxyhaemoglobin as a function of pH. (Adapted from I. D. Campbell and R. A. Dwek, *Biological spectroscopy*, Benjamin/Cummings, Menlo Park, California, 1984, p. 161.)

$[HisH^+] = [His]$, i.e. when the pH equals the pK_a of the imidazole group. Fig. 2.13 shows the pH-dependence of the chemical shift of H2 of one of the histidines (His β146) in the oxy and deoxy forms of haemoglobin, the protein responsible for oxygen transport in blood. The pK_a of His β146 in the deoxy form is higher by about 1 pH unit due to the stabilization of the $HisH^+$ form by the CO_2^- group of a nearby aspartate (Asp β94). These two groups are brought into close proximity by the conformational changes in the protein that accompany deoxygenation. The interaction of His β146 and Asp β94 is partially responsible for the pH-dependence of the oxygen affinity of haemoglobin (the 'Bohr effect').

2.3 Origin of chemical shifts

A magnetic field can induce two kinds of electronic current in a molecule: *diamagnetic* and *paramagnetic* (a diamagnetic material is one in which the magnetization induced by an external field acts so as to *oppose* that field; in a paramagnetic material the induced magnetization *augments* the external field). Diamagnetic and paramagnetic currents flow in opposite directions and give rise to nuclear *shielding* and *deshielding* respectively. The shielding constant may therefore be written as a sum of diamagnetic and paramagnetic contributions:

$$\sigma = \sigma_d + \sigma_p \tag{2.9}$$

with $\sigma_d > 0$ and $\sigma_p < 0$.

Diamagnetic currents arise from the circulation of electrons *within* atomic or molecular orbitals around the direction of the external field $\boldsymbol{B}_0$ (Fig. 2.2). The current so induced generates a small local field opposed to $\boldsymbol{B}_0$. The magnitude of the diamagnetic current is determined by the *ground state* electronic wavefunction of the atom or molecule, depends sensitively on the electron density close to the nucleus, and provides the only contribution to σ for spherical, closed-shell atoms. σ_d is fairly easy to calculate for atoms and varies strongly with the number of electrons: 17.8 ppm for hydrogen, 261 ppm for carbon, 961 ppm for phosphorus, rising to about 10,000 ppm for atoms in the fifth row of the periodic table.

Paramagnetic currents also arise from the movement of electrons within molecules, but by a more circuitous route. Imagine a somewhat artificial molecule with just two electronic states: a ground state comprising an atomic p_x orbital containing two electrons with paired spins, and an unoccupied, higher energy, excited state that resembles a p_y orbital (Fig. 2.14). An external magnetic field directed along the *z*-axis distorts the wavefunction of the ground state by mixing into it a small fraction of the excited state wavefunction. In this way, the field partially overcomes the energy gap between p_x and p_y, which would otherwise keep the electrons locked in p_x, and so creates a path for electrons to circulate in the *xy*-plane (Fig. 2.14). This induced current generates a magnetic field which (it turns out) *augments* the external field and *deshields* a nucleus at the centre of the electron density.

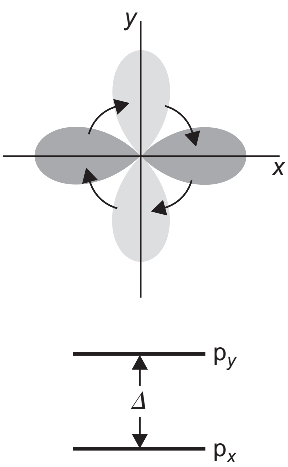

Fig. 2.14 The circulation of electronic charge brought about by the mixing of electronic wavefunctions by a magnetic field. This paramagnetic current generates a small local magnetic field that deshields the nucleus at the centre of the electron density.

The extent of paramagnetic deshielding is clearly linked to the energy gaps involved: other things being equal, low-lying excited states should make a greater contribution than higher energy states. Theory suggests that σ_p should be approximately inversely proportional to Δ, the average excitation energy. The paramagnetic contribution σ_p is also related to the distance R between the nucleus and its surrounding electrons. Since the magnetic field at the centre of a small current loop is proportional to the inverse cube of its radius, we can expect a similar dependence for σ_p. So, very roughly,

$$\sigma_p \propto -\frac{1}{\Delta}\left\langle \frac{1}{R^3} \right\rangle \tag{2.10}$$

where $\langle\cdots\rangle$ indicates an average over the local electron distribution.

σ_p vanishes for a molecule with an axially symmetric local electron distribution (for instance, the π electrons in acetylene) when the external magnetic field is parallel to the symmetry axis. Similarly there is no paramagnetic contribution to the chemical shifts of atoms. The theory of diamagnetic and paramagnetic currents and the chemical shifts they generate is described by Atkins and Friedman (2011).

2.4 **Contributions to nuclear shielding**

It will be clear from the previous section that chemical shifts are sensitive to subtle changes in electronic structure and that calculating nuclear shielding constants from first principles is unlikely to be straightforward. For example, two isotopologues of carbon monoxide, $^{13}C^{16}O$ and $^{13}C^{17}O$, have ^{13}C chemical shifts that differ by 0.025 ppm. This small but measurable difference arises because the average bond length of $^{13}C^{16}O$ is 0.005% longer than that of $^{13}C^{17}O$ (as a result of the mass-dependence of the vibrational frequency and the anharmonicity of the potential energy). Nevertheless, sophisticated *ab initio* electronic structure calculations, based on the fundamental assumptions of quantum mechanics, can now predict chemical shifts that are often in good agreement with experimental measurements. Such calculations are proving to be extremely useful for interpreting NMR spectra (e.g. Bonhomme *et al.* (2012)).

However, as we saw in Section 2.2, it is often not necessary to explain chemical shifts beyond the level of empirical correlations with structure (Fig. 2.12). Despite the complexities alluded to above, chemical shift differences *can* sometimes be traced back to straightforward changes in electron density or excited state energies. We explore these correlations in the following paragraphs.

It will prove useful to divide the nuclear shielding constant σ, arbitrarily, into four parts:

$$\begin{aligned}\sigma = {} & \text{local diamagnetic shielding} \\ & + \text{local paramagnetic shielding} \\ & + \text{shielding due to remote currents} \\ & + \text{other sources of shielding.}\end{aligned} \tag{2.11}$$

The first two are contributions from the electrons in the *immediate* vicinity of the nucleus, i.e. from electrons circulating around it. The third term accounts

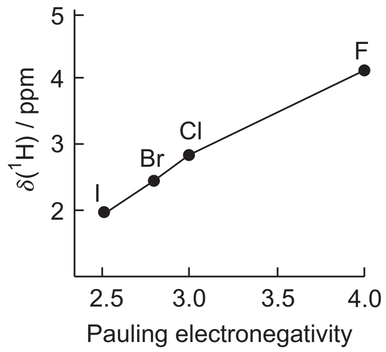

Fig. 2.15 ^1H chemical shifts of methyl halides plotted against the Pauling electronegativity of the halogen.

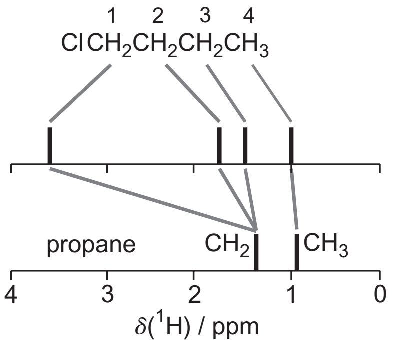

Fig. 2.16 Comparison of the ^1H chemical shifts of 1-chlorobutane and propane.

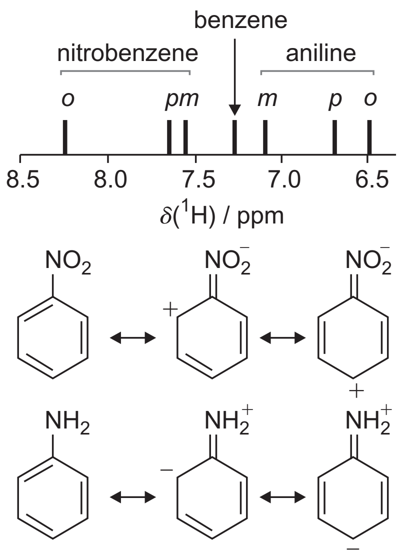

Fig. 2.17 Chemical shifts of the *ortho*, *meta* and *para* protons of aniline and nitrobenzene, together with resonance structures which account for the larger shielding/deshielding of the *ortho* and *para* protons compared to the *meta* proton.

for the diamagnetic and paramagnetic effects of electrons circulating around other (nearby) nuclei. The final part includes the effects of local electric fields, hydrogen bonds, solvent interactions, electron spins, etc. which, though diamagnetic or paramagnetic in origin, are more conveniently discussed separately. The remainder of this chapter gives a few illustrations of each of these contributions to σ.

Local diamagnetic shifts

The contributions to chemical shifts from local diamagnetic currents are strongly dependent on the electron density around the nucleus: the larger the electron density, the greater the shielding and the smaller the chemical shift, δ.

The ^1H chemical shifts of the methyl halides (Fig. 2.15) may readily be understood in these terms. As the electronegativity of the halogen increases, going from iodine to fluorine, electron density is withdrawn from the methyl group, deshielding the protons. Indeed there is a linear correlation between the ^1H chemical shifts and the Pauling electronegativities of the halogens. Methane, which lacks an electron withdrawing group, has a substantially smaller chemical shift (0.13 ppm) than methyl iodide. Electropositive substituents increase the shielding still further, e.g. 0.0 ppm (by definition) for tetramethylsilane.

The deshielding effect of electronegative atoms is fairly short range, as illustrated in Fig. 2.16. Relative to the CH_2 group in propane, the C1 protons of 1-chlorobutane are strongly deshielded; the effect on the C2 and C3 protons is much smaller, but still measurable. The terminal methyl group (C4), four carbons away from the chlorine, is essentially unaffected by the substituent, as judged by its chemical shift relative to the methyl protons in propane.

Similar behaviour is found for monosubstituted benzenes (Fig. 2.17). Groups with electron withdrawing mesomeric effects, NO_2 and CN for example, deshield the ring protons, while electron donating groups, such as NH_2 and OCH_3, result in shielding. The shielding/deshielding is most pronounced for the protons *ortho* and *para* to the substituent, an effect that can be rationalized by means of the resonance structures shown in the figure.

Local paramagnetic shifts

The Δ variation of σ_p (eqn 2.10) is nicely illustrated by the ^{59}Co chemical shifts of octahedral cobalt complexes. The five 3d orbitals of the cobalt(III) ion are split by the octahedral field of the ligands into a set of three degenerate t_{2g} orbitals and a pair of degenerate e_g orbitals, Fig. 2.18. The ground state corresponds to the $(t_{2g})^6$ electronic configuration. The four excited states that arise from the first excited configuration, $(t_{2g})^5(e_g)^1$, all have energies similar to the ligand field splitting, Δ. As shown in Fig. 2.18, there is a remarkably good correlation between the ^{59}Co chemical shift and the wavelength of the lowest energy absorption band which is roughly proportional to $1/\Delta$. Ligands such as carbonate, oxalate, and acetylacetonate which produce small ligand field splittings give large paramagnetic deshielding and hence large chemical shifts δ.

The ^{13}C chemical shifts of monosubstituted benzenes provide a good example of the dependence of σ_p on $\langle R^{-3} \rangle$ (eqn 2.10). As shown in Fig. 2.19, the *para* carbon is deshielded by electron withdrawing substituents (e.g. NO_2) and shielded by electron releasing groups (e.g. NH_2). Although this is the same trend observed for the ^1H shifts in these compounds, the effect is paramagnetic rather than diamagnetic in origin. Electron donating groups delocalize their lone pairs into the ring and increase the electron density at the *ortho* and *para* carbons. The increased electron repulsion causes the orbitals around these atoms to *expand*, reducing $\langle R^{-3} \rangle$ and hence δ.

At this point we can see why the chemical shift range of ^1H is so small compared to other nuclei (~10 ppm for ^1H; ~200 ppm for ^{13}C; ~300 ppm for ^{19}F, ~500 ppm for ^{31}P, etc.). Local diamagnetic and local paramagnetic currents make only modest contributions because of the low electron density and high electronic excitation energy of the hydrogen atom. Indeed, ^1H chemical shifts are often more strongly influenced by the diamagnetic and paramagnetic currents in *neighbouring groups* of atoms which have larger electron densities and lower excitation energies, as we shall now see.

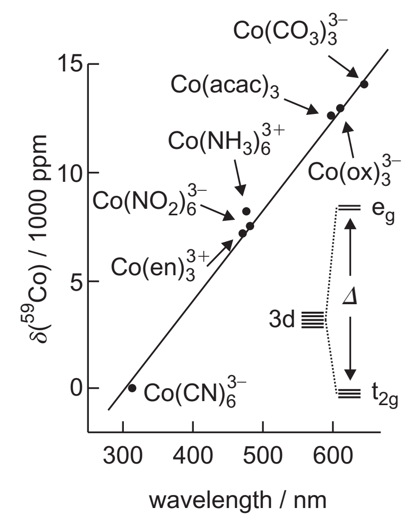

Fig. 2.18 ^{59}Co chemical shifts (relative to $Co(CN)_6^{3-}$) of octahedral cobalt complexes plotted against the wavelength of the first electronic absorption band. en = ethylenediamine; ox = oxalate; acac = acetylacetonate. (Adapted from R. Freeman, G. R. Murray, and R. E. Richards, *Proc. R. Soc. A*, **242** (1957) 455.)

Neighbouring groups

To understand the (de)shielding of a nucleus caused by the motions of electrons in nearby groups of atoms, we take a specific example: an acetylene-substituted phenanthrene molecule (Fig. 2.20) in which the proton beside the C≡C bond is deshielded by 1.7 ppm compared to phenanthrene itself.

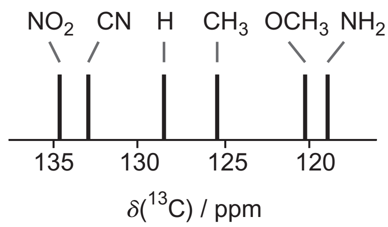

Fig. 2.19 ^{13}C chemical shifts of the *para* carbons in monosubstituted benzenes.

The magnetic field of the spectrometer ($\boldsymbol{B}_0$) induces electronic currents in the π electrons of the C≡C group which generate a local magnetic field. Let us suppose, for simplicity, that this small induced field has the same general form as the magnetic field that would be produced by a *magnetic dipole* μ (i.e. a microscopic bar magnet) sitting at the centre of the C≡C bond. μ is either parallel or antiparallel to $\boldsymbol{B}_0$ according to whether the induced current is paramagnetic or diamagnetic, respectively. Fig. 2.21 shows two orientations of the phenanthrene molecule, with the acetylene group aligned perpendicular (a) and parallel (b) to $\boldsymbol{B}_0$. The dipolar field lines generated by μ are drawn on the assumption that the diamagnetic currents are small (as is actually the case for acetylene). From the directions of the magnetic field lines, the phenanthrene proton should be deshielded in (a) and shielded in (b). Now we need to average over the random orientations of the molecule in solution which will inevitably cause (at least) partial cancellation of the shielding and deshielding effects shown in Fig. 2.21. In fact the cancellation would be *exact* if μ were the same for all orientations of the molecule (Section 3.8). But the C≡C bond is magnetically anisotropic and currents are 'easier' to induce in some directions than in others. When the C≡C bond is parallel to $\boldsymbol{B}_0$ there is no paramagnetic current induced in the triple bond because of its cylindrical symmetry (Section 2.3). The diamagnetic π-electron currents are small for all orientations of the molecule so that the dominant effect occurs for orientation (a) in which the induced paramagnetic current is large. The result is that the phenanthrene proton is deshielded.

The magnetic field arising from a magnetic dipole is described in Appendix A.

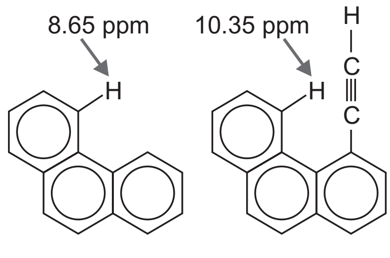

Fig. 2.20 Deshielding due to the magnetic anisotropy of a C≡C bond.

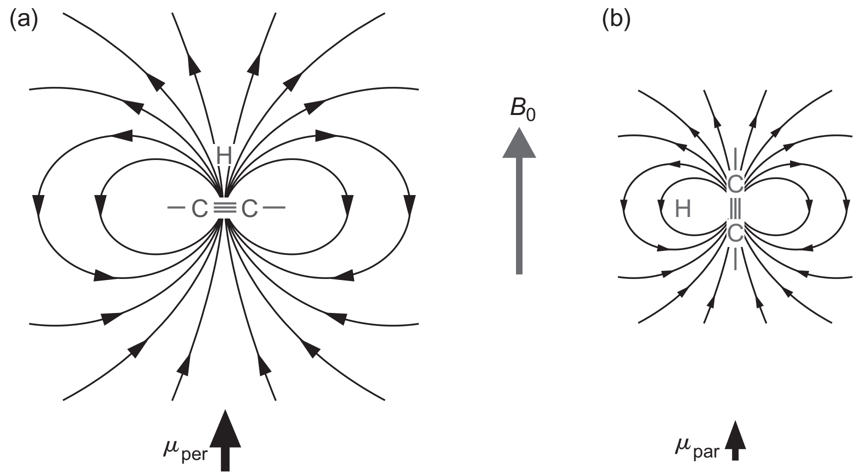

Fig. 2.21 Dipolar magnetic field lines (see Appendix A) generated by an induced magnetic moment at the centre of the acetylene group in the substituted phenanthrene shown in Fig. 2.20 (only the C≡C bond and the nearby phenanthrene proton are shown.). The proton is deshielded in orientation (a) and shielded in orientation (b) by the induced magnetic field. The opposite effect is expected for the acetylenic proton (not shown). The magnetic moment induced in the C≡C bond is larger in the perpendicular orientation (per) than the parallel orientation (par).

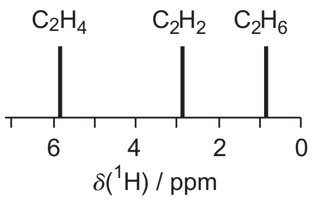

Fig. 2.22 ^1H chemical shifts of C_2H_6, C_2H_4, and C_2H_2.

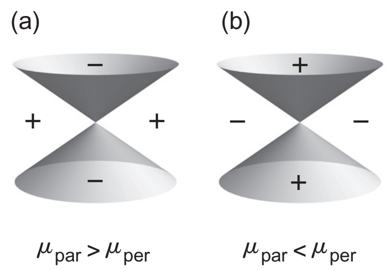

Fig. 2.23 Regions of shielding (+) and deshielding (−) due to neighbouring group magnetic anisotropy, for (a) $\mu_{par} > \mu_{per}$ and (b) $\mu_{par} < \mu_{per}$. If the fields generated by the induced magnetic moments were exactly those of a point dipole, the half angle of the cones would be $\theta = 54.7°$ (the so-called *magic angle* at which $3\cos^2\theta = 1$). The axis of the cones coincides with the symmetry axis of the neighbouring group.

This source of chemical shifts is generally referred to as *neighbouring group anisotropy*. The magnitude of the effect depends on the magnetic anisotropy of the neighbouring group itself and not on the nucleus being shielded or deshielded. It is therefore *relatively* more important for protons with their small local diamagnetic and paramagnetic currents than for other nuclei, ^{13}C for instance, which have larger local electron densities and lower excitation energies. Only groups that have very high symmetry, e.g. tetrahedral, have no magnetic anisotropy.

But what about the proton *attached* to the C≡C bond in acetylene? Fig. 2.22 shows the ^1H chemical shifts of acetylene, ethylene, and ethane. Considering the hybridization of the molecular orbitals, one would expect $\delta(C_2H_6) < \delta(C_2H_4) < \delta(C_2H_2)$. As the s-electron character of the σ bonds increases (in the order $sp^3 < sp^2 < sp$) so the bonding electrons should be held more tightly to the carbons, removing electron density from the hydrogen atoms and deshielding the protons. The observed order of shifts arises from the *shielding* effect of the π electrons of the triple bond (Fig. 2.21(a) again), and also the neighbouring group effect of the C = C double bond which *deshields* the protons in ethylene.

A simple extension of the above argument leads to the diagrams in Fig. 2.23. Let μ_{par} and μ_{per} be the magnitudes of the induced magnetic moments when the $\boldsymbol{B}_0$ field is respectively parallel and perpendicular to the axis of the neighbouring group which is assumed to have cylindrical symmetry. When (a) $\mu_{par} > \mu_{per}$, a nucleus lying *within* one of the two cones should be deshielded, while a nucleus in the region *outside* the cones should be shielded. The opposite (b) holds when, as in acetylene, $\mu_{par} < \mu_{per}$. In reality, both the angular and radial dependence of the induced field are more complicated than this simple picture would suggest; nevertheless it remains a useful way of thinking about neighbouring group anisotropy, and if approached with caution, can be used to predict the direction, although not the magnitude, of chemical shift differences.

Another instance of the neighbouring group effect occurs in *aromatic* compounds, whose extensive π-electron 'clouds' can support large electronic currents. In molecules such as benzene, the dominant contribution to the magnetic anisotropy comes from the circulation of the π electrons *within* their delocalized molecular orbitals; i.e. the neighbouring group effect is due principally to the *diamagnetic* moment induced when the external field is parallel to the six-fold symmetry axis, as indicated in Fig. 2.24. However, the end result is the same as for acetylene because the induced diamagnetic moment is *opposed* to the external field ($\mu_{par} < 0$), so that the anisotropy ($\mu_{par} - \mu_{per}$) is once again negative. Thus we can anticipate deshielding for nuclei in the plane of the aromatic ring, and shielding for any nuclei above or below the ring.

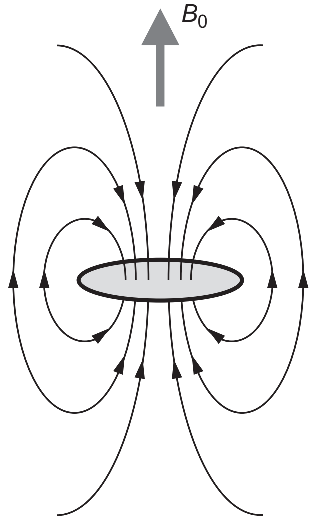

Fig. 2.24 Schematic magnetic field lines arising from the diamagnetic current induced in a benzene ring when the external field is parallel to the six-fold symmetry axis of the ring.

This *ring current shift* is demonstrated clearly by benzene itself, whose ^{1}H chemical shift is + 1.4 ppm relative to the olefinic protons in cyclohexa-1,3-diene, Fig. 2.25(a). A more interesting example is the *trans*-dimethyl-substituted dihydropyrene in Fig. 2.25(b) which, with 14 π-electrons, is aromatic according to the $4n + 2$ rule ($n = 3$). The ring protons are deshielded, as in benzene, but the methyl groups, which protrude above and below the plane of the molecule, are shielded by more than 5 ppm relative to ethane. (A negative δ value means that the resonance appears in the spectrum to the right of TMS.) As indicated in Fig. 2.24, the methyl protons lie in a region where the induced field *opposes* the external field.

Finally, the planar aromatic molecule [18]-annulene in Fig. 2.25(c), with 18 π-electrons, shows two ^{1}H resonances, one from the 12 strongly deshielded external protons, and one at –2.99 ppm from the six internal protons. The latter set of hydrogen atoms lies within the current loop formed by the circulating π electrons, and as indicated in Fig. 2.24 is shielded by the ring current effect. Note that the chemical shifts of these nuclei cannot, even qualitatively, be described using the point dipole approximation (Fig. 2.23) which predicts deshielding for any nucleus in the plane of the aromatic ring, however close to the centre of the molecule.

Although only C≡C and C=C bonds and aromatic rings have been discussed, neighbouring group effects exist for other functional groups, C–C, C=O, and N=O for example, and have a strong influence on ^{1}H chemical shifts.

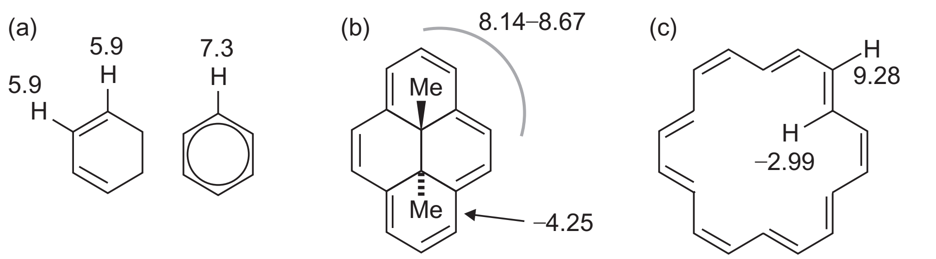

Fig. 2.25 Ring current shifts. ^{1}H chemical shifts (ppm) in: (a) benzene compared to cyclohexa-1,3-diene; (b) *trans*-15,16-dimethyl-15,16-dihydropyrene; (c) [18]-annulene.

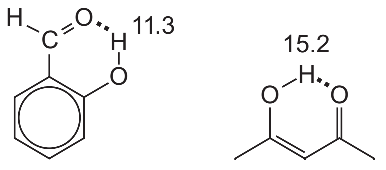

Fig. 2.26 Deshielding due to hydrogen bonding. ^1H chemical shifts (in ppm) in salicylaldehyde and the enol form of acetylacetone.

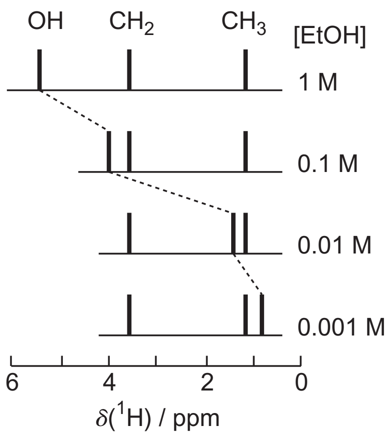

Fig. 2.27 Hydrogen bonding shifts in ethanol, as a function of concentration in CCl_4.

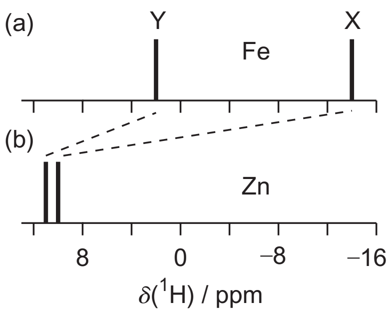

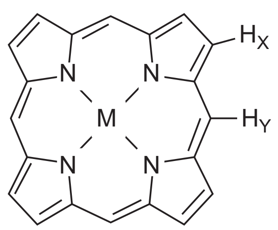

Fig. 2.28 ^1H chemical shifts of the two types of proton (X and Y) in (a) the paramagnetic Fe^{3+} (porphin) CN^- ion and (b) the diamagnetic Zn^{2+} (porphin) ion.

Other sources of chemical shifts

Hydrogen bonding is responsible for some of the largest observed ^1H chemical shifts. Two compounds that form intramolecular hydrogen bonds are shown in Fig. 2.26: in both, the hydrogen-bonded proton is heavily deshielded. Intermolecular hydrogen bonds, which are generally somewhat weaker, produce smaller shifts. For example, the hydroxyl proton resonance of ethanol moves by about −4 ppm when the intermolecular hydrogen bonding is disrupted by dilution in CCl_4 (see Fig. 2.27). The limiting shift of the OH resonance at infinite dilution (~0.8 ppm) is similar to the value for monomeric ethanol in the gas phase (0.55 ppm). Similar changes in the OH chemical shift are found with increasing temperature, which also favours the monomer side of the monomer $\rightleftharpoons$ dimer, trimer,... equilibrium. The origin of the deshielding caused by hydrogen bonding is unclear. Most likely, the strong electric field of the Y atom in X-H$\cdots$Y draws the hydrogen atom slightly away from the electrons in the X–H bond, so reducing the electron density immediately around it.

Chemical shifts are also affected by the local *electric* fields arising from charged or polar groups. These can modify both diamagnetic and paramagnetic currents by polarizing local electron distributions, and by perturbing ground and excited state wavefunctions and energies. Positive charges usually deshield nearby protons, while negative charges often give rise to shielding. For example, the protons on the imidazole side-chain of the amino acid histidine are deshielded by about 1 ppm when the ring is protonated (Fig. 2.13).

Finally, in this far from complete survey, there are the *paramagnetic* shifts produced by electron spins (in this context paramagnetic refers to the permanent magnetic moment of the electron and not to the induced electronic currents discussed above). Unpaired electrons give rise to large dipolar magnetic fields (Appendix A)—the magnetogyric ratio of the electron is 660 times that of the proton—which can result in substantial nuclear shielding/deshielding, as illustrated by the two metal–porphin complexes in Fig. 2.28. The two types of proton in the aromatic ligand, which have large ring current shifts in the diamagnetic Zn^{2+} complex, are heavily shielded in the paramagnetic Fe^{3+} compound.

2.5 Summary

- Nuclei (e.g. protons, ^1H) in molecules have slightly different NMR frequencies, an effect known as the chemical shift.
- Chemical shifts arise from induced electronic currents which shield or deshield the nuclei from the applied magnetic field.
- The chemical shift parameter δ quantifies the extent of nuclear shielding/deshielding.
- The magnitudes of induced diamagnetic and paramagnetic currents can be related to local electron densities and electronic excitation energies.
- Chemical shifts can often be understood by considering the effects of electron donating and withdrawing groups, induced currents in

neighbouring groups, charged or polar groups, hydrogen bonds, and unpaired electrons.

Chemical shifts distinguish nuclei in different environments in molecules and give information on molecular identity and structure.

2.6 Exercises

Answers to the exercises are provided at the back of the book. Full worked solutions are available on the Online Resource Centre at < URL >

1. The ^1H chemical shifts of benzene and dimethylsulphoxide are 7.3 and 2.4 ppm respectively. What is the difference in the ^1H NMR frequencies of the two compounds on a 750 MHz spectrometer?
2. The ^1H Larmor frequency of C_2H_6 exceeds that of C_2H_4 by 3.0 kHz on a spectrometer with a 14.1 T magnet. The chemical shift of C_2H_6 is 0.9 ppm. What is the chemical shift of C_2H_4?
3. Use the data in Fig. 2.18 to estimate the difference in ^{59}Co NMR frequencies of $Co(CN)_6^{3-}$ and $Co(CO_3)_3^{3-}$ in a 9.4 T magnetic field. $[\gamma(^{59}Co) = 1.637 \times 10^6\ T^{-1}\ s^{-1}]$.
4. The following compounds all exhibit a single line in their ^1H NMR spectra. Deduce their structures. (a) $C_6H_4Cl_2$. (b) $C_3H_6Cl_2$. (c) $C_3H_2Cl_6$. (d) $C_3H_4Cl_2$. (e) $C_6H_4O_2$.
5. (a) How many distinct chemical shifts would you expect to find in the ^{13}C spectra of the following isomers of C_5H_{12}: pentane, 2-methylbutane, and 2,2-dimethylpropane? (b) How many distinct chemical shifts would you expect to find in the ^1H spectra of the three isomers of dichlorocyclopropane?
6. ^1H and ^{13}C NMR spectra were recorded for two isomers of $C_3H_2Cl_6$. Both ^{13}C spectra contain peaks at three distinct chemical shifts. Isomer 1 has one distinct ^1H chemical shift and isomer 2 has two. (a) Deduce the structures of the two compounds. (b) Predict the number of chemical shifts in the ^1H and ^{13}C spectra of the other two isomers of $C_3H_2Cl_6$.
7. The lowest energy electronic transitions in alkanes and alkenes are approximately 10 eV and 8 eV respectively. Predict whether saturated (sp^3) or unsaturated (sp^2) ^{13}C nuclei have larger chemical shifts.
8. Predict which of the following compounds has the highest and which the lowest ^1H chemical shift: CH_3Br, CH_2Br_2, $CHBr_3$.
9. Predict which of the ortho, meta, and para protons in methoxybenzene has the highest and which the lowest ^1H chemical shift.
10. The ring current shift of a ^1H nucleus close to a benzene ring is approximately proportional to $(1 - 3\cos^2\theta)/r^3$ where θ is the angle between a vector perpendicular to the plane of the ring and the vector that connects the ^1H to the centre of the ring. r is the distance of the ^1H from the centre of the ring. The ring current shift of the protons in benzene is $+2$ ppm. The C–C and C–H bond lengths in benzene are 140 and 110 pm, respectively. A ^1H immediately above the centre of the ring $\theta = 0$ has a ring current shift of –2 ppm. What is its distance from the centre of the ring?